Electronic Supplementary Information

Asymmetric zinc porphyrin-sensitized nanosized TiO_2 for efficient visible-light-driven CO_2 photoreduction to CO/CH_4

Kan Li, Li Lin, Tianyou Peng*, Yingying Guo, Renjie Li and Jing Zhang
College of Chemistry and Molecular Science, Wuhan University, Wuhan 430072, P. R. China
E-mail: typeng@whu.edu.cn

EXPERIMENTAL SECTION

Material preparation

TiO_2 preparation: Typically, $TiCl_4$ (2.85 g, ~15 mmol) was dropped into absolute ethanol (40 g), and then urea (95.0 g) was added with continually stirring. Immediately following the urea dispersed, sodium lactate solution (5.0 mL, ~60%) was added dropwise, and then the mixture was transferred into a Teflon-lined autoclave (total volume of 100 mL), which was sealed and kept at 200°C for 20 h and then cooled to room temperature naturally. The precipitate was centrifugally separated and washed with distilled water and absolute ethanol for several times. The product dried at 70°C was calcined in air for 3 h at 500°C with a heating rate of 2°C min^{-1}.

Porphyrin (H_2Py) synthesis: H_2Py (5-(4-carboxyphenyl)-10,15,20-tri(3-pyridyl)porphyrin) was synthesized in advance as shown in Fig. S1. 3-pyridylcarboxaldehyde (803 mg, 7.5 mmol) and 4-carboxy-benzaldehyde (375 mg, 2.5 mmol) were dissolved in propionic acid (100 mL) and brought to reflux at 140°C, and then pyrrole (0.67 mg, 10 mmol) was added, and continued reflux for another 8 h. The resultant back crude was filtered off after adding distilled water (100 mL) under vacuum, then purified by silica gel column chromatography using dichloromethane/ methanol (90:10, v/v) as solvent. The dark purple solid was then purified by re-crystallization from a dichloromethane/hexane mixture to obtain H_2Py (Yield: 107 mg, 6.5%). TOF-MS (m/z) calcd. for $C_{42}H_{27}N_7O_2$ $[M+H]^+$ 661.71, found 662.58. ^1H NMR (DMSO-d_6, 300 MHz): δ=13.2 (1H), 9.40 (2H), 9.06-9.08 (2H), 8.80-8.90 (7H), 8.60-8.70 (3H), 8.34-8.49 (5H), 7.90-8.04 (5H), -2.50 (2H).

Zinc (II) porphyrin (ZnPy) synthesis: ZnPy was prepared by refluxing H_2Py (50 mg, 0.076 mmol) and $Zn(OAc)_2{\cdot}2H_2O$ (67 mg, 0.304 mmol) in DMF (10 mL) for 5 h at 100°C as shown in Fig. S1. The solvent was removed after 20 mL distilled water was added to the reaction mixture. The precipitate was centrifuged, washed three times with distilled water and dried overnight

under vacuum to obtain ZnPy. (Yield: 44 mg, 81.5%). TOF-MS (m/z) calcd. for $ZnC_{42}H_{25}N_7O_2$ $[M+H]^+$ 723.14, found 723.26. ^1H NMR (DMSO-d_6, 300 MHz): δ=9.33 (2H), 9.00-9.02 (2H), 8.81-8.85 (7H), 8.55-8.65 (3H), 8.30-8.40 (5H), 7.85-8.00 (5H) (H in –COOH is not been found).

ZnPy-TiO_2 preparation: ZnPy-sensitized TiO_2 (ZnPy-TiO_2) was prepared by an impregnation method. Typically, the above TiO_2 product (0.20 g) was mixed with ZnPy solution (20 mL, varied with the dye-loading level) under stirring for 12 h, and then centrifugally separated and dried in vacuum at 70°C overnight to obtain ZnPy-TiO_2. The dye-loaded amount was calculated based on the absorbance difference of the ZnPy solution before/after the dye sensitization process.

Material characterization

X-ray powder diffraction (XRD) pattern was obtained by Miniflex 600 X-ray diffractometer with Cu Kα irradiation (λ = 0.154 nm) at 40 kV and 15 mA and a scan rate of 4^o min^{-1} in the range of $10^o \leq 2\theta \leq 50^o$. Raman spectrum was measured on a RM-1000 Renishaw Confocal Raman Microspectroscopy with scanning from 100 cm^{-1} to 1200 cm^{-1} and 10 s of CCD exposure time. Nitrogen adsorption-desorption isotherm at 77 K was measured on a Micrometrics ASAP 2010 system after sample were degassed at 120°C. The morphology was observed with Zeiss-Sigma field emission scanning electron microscope (FESEM), and high-resolution transmission electron microscopy (HRTEM) observation was conducted on a LaB6 JEM-2100(HR) electron microscope (JEOL Ltd.) working at 200 kV.

^1H NMR spectra were recorded on a 300 MHz Bruker DPX 300 spectrometer in DMSO-d_6. MALDI-TOF-MS spectra were taken on a Bruker BIFLEX III ultrahigh resolution Fourier transform ion cyclotron resonance (FT-ICR) mass spectrometer with alpha-cyano-4-hydroxy-cinnamic acid as a matrix. UV-Vis absorption spectra were recorded on a TU-1810 spectrophotometer with scanning from 250 to 900 nm. Fluorescence spectra were recorded on a K2 ISIS spectrometer. Fourier transform infrared (FTIR) spectrum was recorded by using a Nicolet iS10 spectrometer (Thermo Electron).

UV-vis diffuse reflectance absorption spectra (DRS) were obtained by a Shimadzu UV-3600 spectrophotometer equipped with an integrating sphere with $BaSO_4$ as the reference sample. Photoluminescence (PL) spectrum was determined by using a Hitachi F-4500 fluorescence spectrophotometer. Time-resolved photoluminescence (PL) spectra were recorded by a Multifunction Steady State and Transient State Fluorescence Spectrometer (FES920, Edinburgh Instruments) at 398 nm with 375 nm excitation.

In situ DRIFTS IR spectra were recorded on a Nicolet iS50 spectrometer (Thermo Electron)

equipped with a liquid nitrogen cooled HgCdTe (MCT/A) detector. The spectra in absorbance units, and acquired with a resolution of 4 cm^{-1} by using 256 scans. Typically, 40 mg catalyst was uniformly dispersed onto the DRIFTS accessory, which was then thoroughly vacuum-treated to remove air completely, and then pure CO_2 (99.999%) gas and H_2O vapor were introduced into the reactor until 1 atm and then maintained for 20 min before collecting the IR spectra.

Photocatalytic and photoelectrochemcial property measurement

Photocatalytic CO_2 reduction was carried out in a home-made gas-closed circulation system operated under a 300 W Xe-lamp irradiation. Typically, catalyst (60 mg) was uniformly dispersed onto the watch-glass with an area of ~28 cm^2, which was then put in the reaction cell (Pyrex glass) with a total volume of 500 mL. Prior to the light irradiation, the above system was thoroughly vacuum-treated to completely remove air. CO_2 and H_2O vapor were produced from the reaction of $NaHCO_3$ (1.00 g, introduced into the reactor before being sealed) and H_2SO_4 solution (5.0 mL, 4.0 M, introduced into the reactor *via* a syringe after the vacuum treatment). During irradiation, 2 mL gas was taken from the reactor at regular intervals (1 h) for the gas concentration analysis using a gas chromatograph (SP-7820, TDX-01 column, Rainbow chemical instrument Co. Ltd., China) equipped with a flame ionized detector (FID) and methanizer. The produced gases were calibrated with a standard gas mixture and their identity determined using the retention time.

For the stability test of catalyst (1.0% ZnPy-TiO_2), the watch-glass with irradiated catalyst was moved out of the reaction cell after each run, and then dried in vacuum at 60^{o}C for 3 h to remove the physical adsorbed H_2O and CO_2. The watch-glass containing the recycled catalyst was then used the subsequent CO_2 photoreduction process as mentioned above.

For obtaining the photocurrent and electrochemical impedance spectra (EIS), working electrodes were prepared as follows: sample (0.2 g) was ground with ethanol (0.8 g), the resultant slurry was then coated onto a FTO glass by the doctor blade method. These electrodes were dried and calcined at 500^{o}C for 1 h. All electrodes tested had a similar film thickness. Photocurrents were measured using an electrochemical analyzer (CHI 618C Instruments) in a standard three electrode system by using the prepared film as the working electrodes (an effective area of 1 cm^2), a Pt flake as the counter electrode, and Ag/AgCl as the reference electrode. Bias potential applied on the working electrode was 0.5 V. A 300 W Xe-lamp (CHF-XM 500, Beijing Trusttech Co. Ltd., China) served as a light source to irradiate the working electrode from the back side. A 1.0 M Na_2SO_4 solution was used as the electrolyte.

FIGURES AND TABLES

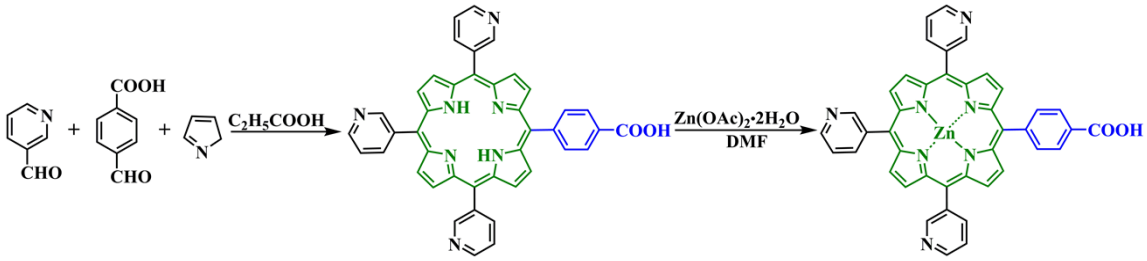

Fig. S1 Synthetic route of H_2Py and ZnPy.

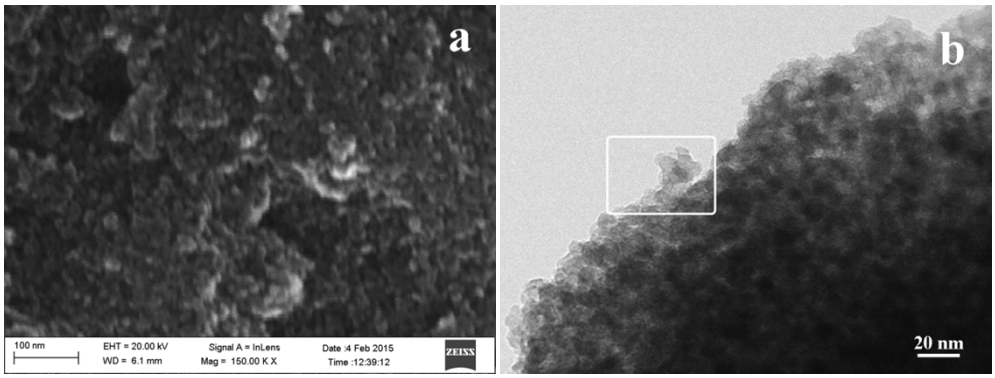

Fig. S2 FESEM (a) and TEM (b) images of the synthesized TiO_2 nanoparticles.

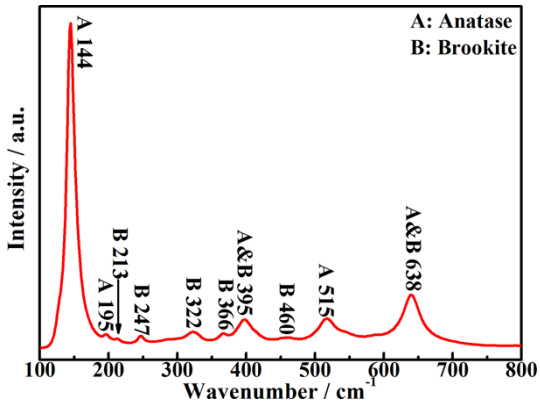

Fig. S3 Raman spectrum of the synthesized TiO_2 nanoparticles.

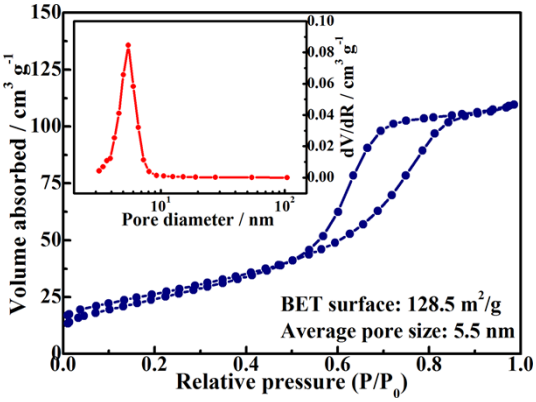

Fig. S4 N_2 adsorption-desorption isotherm and Barrett-Joyner-Halenda (BJH) pore size distribution plot (inset) of the synthesized TiO_2 nanoparticles.

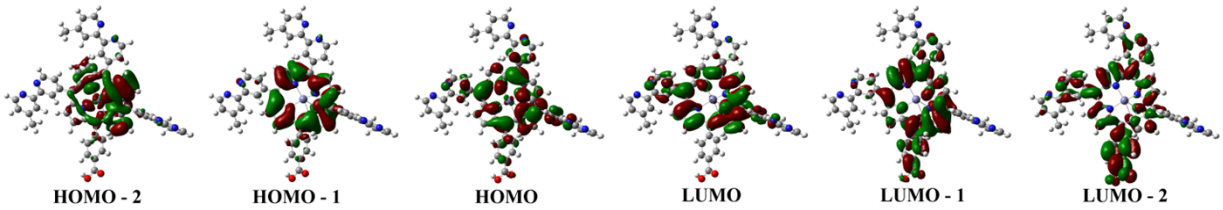

Fig. S5 The frontier orbitals of ZnPy obtained from the DFT calculation, full optimized at B3LYP/6-31g level.

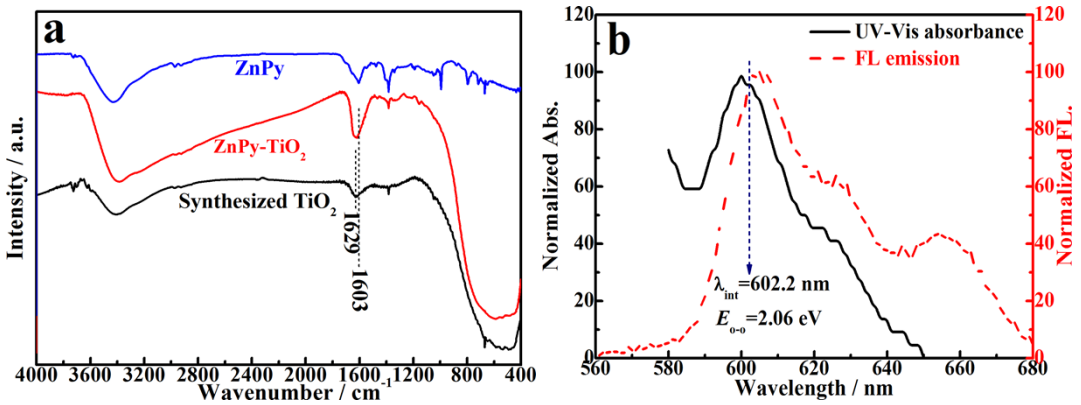

Fig. S6 (a) FTIR spectra of ZnPy, TiO_2 and ZnPy-TiO_2; (b) the normalized UV-Vis absorption and fluorescence emission spectra of ZnPy.

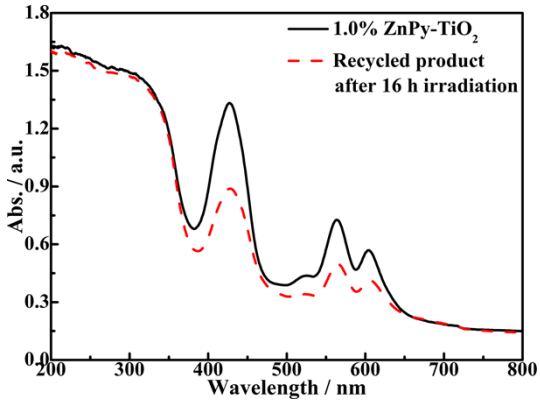

Fig. S7 UV-vis diffuse reflection absorption spectra (DRS) of 1.0% ZnPy-TiO_2 and its recycled product after 16 h light irradiation.

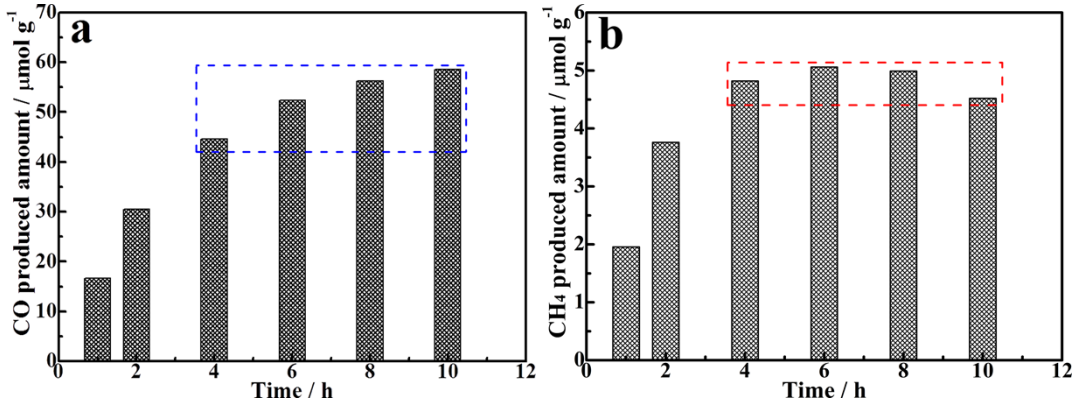

Fig. S8 Typical CO (a) and CH_4 (b) produced amount over 1.0% ZnPy-TiO_2 for 1, 2, 4, 6, 8, and 10 h continuous irradiation under λ≥420 nm light.

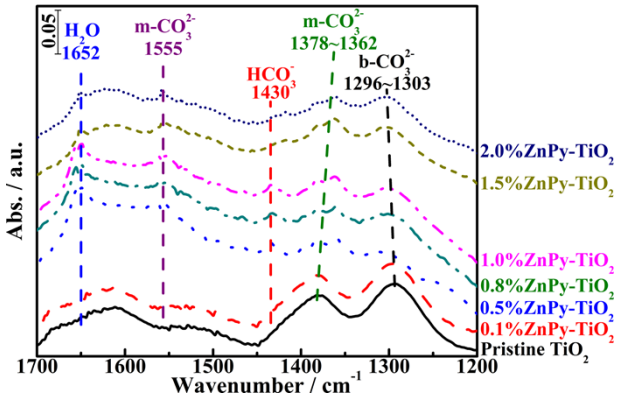

Fig. S9 *In situ* DRIFTS IR spectra of CO_2 interactions with the synthesized TiO_2 and 1.0% ZnPy-TiO_2.

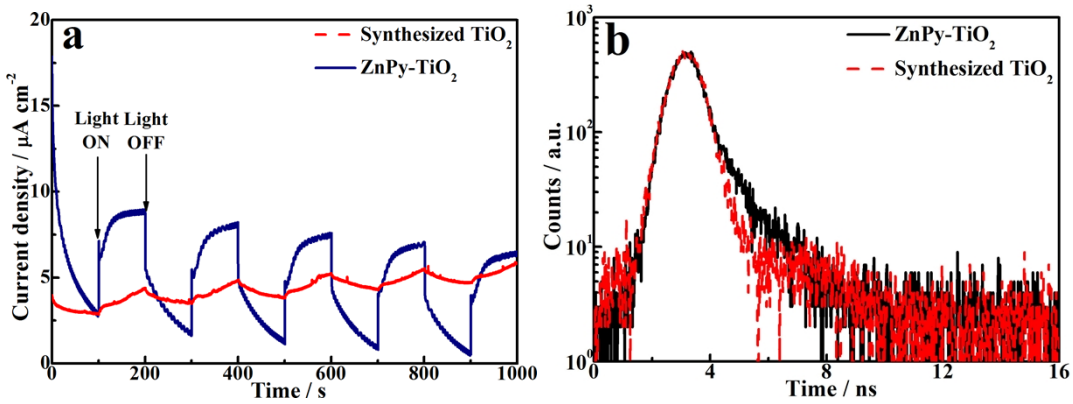

Fig. S10 Photocurrent-time curves (a) and time-resolved PL spectra (b) of the synthesized TiO_2 and 1.0% ZnPy-TiO_2.

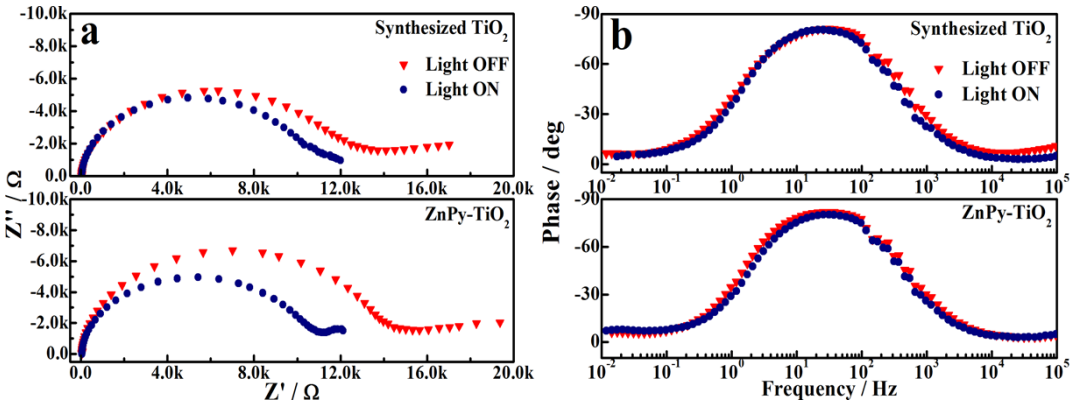

Fig. S11 Electrochemical impedance spectra (EIS) spectra of the synthesized TiO_2 and 1.0% ZnPy-TiO_2. Nyquist (a) and Bode (b) plots.

Table S1 Spectral, electrochemical and DFT calculated data of ZnPy.

Dye	λ_{max} / nm	ε / *10^5 L mol^{-1} cm^{-1}	E_{ox} / V(*vs.* SCE)	E_{red} / V(*vs.* SCE)	$E_{0\text{-}0}$ / eV	E^* / V	HOMO[c] / V	LUMO[c] / V
ZnPy	420	2.00	0.95[a]	-0.99[a]	2.06	-1.11[a]	1.16[a]/0.72[b]	-0.90[a]/-1.63[b]

[a] Data are obtained from the electrochemical measurements.
[b] Data are obtained from the DFT calculation.
[c] HOMO and LUMO states are *vs.* NHE.

Table S2 CO_2 photoreduction activity and the TCEN value of ZnPy-TiO_2.

Catalysts	Dye-sensitized level [a]/ %	CO produced rate / μmol g^{-1} h^{-1}	CH_4 produced rate [b] / μmol g^{-1} h^{-1}	TCEN / μmol g^{-1} h^{-1}
Pristine TiO_2	0	0	0	0
0.1% ZnPy-TiO_2	0.08	1.07	0	2.15
0.5% ZnPy-TiO_2	0.42	3.55	Trace	7.09
0.8% ZnPy-TiO_2	0.70	6.89	0.87	20.70
1.0% ZnPy-TiO_2	0.86	8.07	1.01	24.17
1.5% ZnPy-TiO_2	1.23	7.74	0.48	19.28
2.0% ZnPy-TiO_2	1.51	5.96	Trace	11.92

[a] Dye-sensitized level is determined by the concentration difference of the ZnPy solution before/after sensitization.

[b] Trace means that CH_4 produced rate cannot measure quantitatively.

Table S3 Comparison with other photocatalytic systems

Catalyst	Light source	Reaction condition	Yield (Product) /μmol g^{-1} h^{-1}	TCEN /μmol g^{-1} h^{-1}	Ref.
TiO_2	500 W tungsten-halogen lamp	0.1 M NaOH solution with bubbled CO_2	32.1/10.58/1.67 ($HCOOH/CO/CH_4$)	98.7	1
1.0% ZnPc-TiO_2	500 W tungsten-halogen lamp	0.1 M NaOH solution with bubbled CO_2	87.9/15.4/7.65 ($HCOOH/CO/CH_4$)	267.9	
u-g-C_3N_4	300 W Xe-lamp, λ>420 nm	1.0 M NaOH solution with saturated CO_2	6.28/4.51 (CH_3OH/ C_2H_5OH)	91.8	2
Lamellar $BiVO_4$	300 W Xe-lamp	1.0 M NaOH solution with saturated CO_2	5.52 (CH_3OH)	33.12	3
	300 W Xe-lamp, λ>420 nm	1.0 M NaOH solution with saturated CO_2	3.76 (CH_3OH)	22.56	
1.0% Au-$NaTaO_3$	200 W Hg-Xe lamp	CO_2/H_2O vapor	0.17/0.04 (CO/CH_4)	0.634	4
TiO_2 with exposed {001}/{101} facets	300 W Xe-lamp	CO_2/H_2O vapor	1.35 (CH_4)	10.8	5
1.0% Pt-TiO_2 with exposed {001} facets	300 W Xe-lamp	CO_2/H_2O vapor	2.60 (CH_4)	20.8	6
1.0% ZnPy-TiO_2	300 W Xe-lamp, λ>420 nm	CO_2/H_2O vapor	8.07/1.01 (CO/CH_4)	24.17	This work

Table S4 Photoelectrochemical parameters derived from EIS and time-resolved PL spectra.

Catalyst	Irradiation condition	R_s / Ω cm^2	R_1 / Ω cm^2	R_2 / kΩ cm^2	τ_n [a] / ms	τ_n' [b] / ns
Pristine TiO_2	OFF	21.4	6.5	13.5	5.05	1.55
	ON	32.7	2.0	11.1	6.19	
ZnPy-TiO_2	OFF	32.2	7.1	14.8	6.19	7.78
	ON	48.5	2.3	11.4	6.19	

[a] τ_n is calculated from the EIS Bode plot.

[b] τ_n' is the photoinduced electron lifetime calculated from the time-resolved PL spectra.

RESULTS AND DISCUSSIONS

Total consumed electron number (TCEN) calculation

In the present gas phase CO_2 photoreduction system, the reaction of CO_2 conversion to CH_4 involves 8 electrons transfer process, while the reaction for the CO production relates to 2 electrons transfer process as follows:

$$CO_2 + 2H^+ + 2e^- \rightarrow CO + H_2O$$

$$CO_2 + 8H^+ + 8e^- \rightarrow CH_4 + H_2O$$

Fig. 3a shows the effects of the ZnPy-loading level on the photocatalytic CO/CH_4 production activities during the initial 2 h light irradiation, and the corresponding overall photoactivity for the CO/CH_4 generation over ZnPy-TiO_2 can be estimated with total consumed electron number (TCEN), which is calculated with Eqn. (1).[4,7,8]

$$\text{TCEN} = \frac{(2c_{CO} + 8c_{CH_4}) \times V_{reactor}}{m_{cat.} \times t_{irr.}} \qquad (1)$$

Where, TCEN is the total consumed electron number for the CO/CH_4 generation. $V_{reactor}$ is the reactor volume (0.5 L). $t_{irr.}$ is the irradiation time. $m_{cat.}$ is the catalyst dosage (60 mg). c_{CO} and c_{CH_4} are the produced CO and CH_4 concentration, respectively.

ZnPy energy level measurement

The thermodynamic practicability is an important aspect in a dye-sensitized semiconductor, the electrochemical behaviors of the synthesized ZnPy was investigated by using cyclic voltammetry (CV), and the corresponding results and calculated HOMO (E_{HOMO} = -(E_{ox} + 4.71) eV, and then converted to *vs.* NHE as shown in Table S1) and LUMO (E^*= (E_{ox}-E_{o-o}) eV, and also converted to *vs.* NHE) levels of ZnPy are shown in Table S1 according to the previous method reported in literatures.[9,10] Among which, E_{ox} is obtained from the CV curve; and E_{o-o} is obtained from the intersection of normalized absorption and emission spectra of the ZnPy dye as shown in Fig. S6b. As can be seen from Table S1, the E^* value of ZnPy is sufficiently negative as compared with the CB of TiO_2 (-0.53 V *vs*. NHE).[9,10] Therefore, the electrons of the excited ZnPy molecules can be injected into the CB of TiO_2, which then resulting in the CO_2 photoreduction to carbon fuels.

Comparison with the other CO_2 photocatalytic systems

Generally, CO_2 photoreduction over catalyst can be conducted in liquid or gas phase

photoreaction system. In liquid phase system, the catalyst can be dispersed uniformly and well attached with those dissolved CO_2 species, such as carbonate (CO_3^{2-}), bicarbonate (HCO_3^-) and carbon dioxide (CO_2 and H_2CO_3), and thus the photocatalytic activity of CO_2 conversion is usually higher than that of the gas phase system as shown in Table. S3. However, it is difficult to determine the initial reactants due to the ionization equilibrium among CO_3^{2-}, HCO_3^-, CO_2 and H_2CO_3 in the liquid phase system, and thus gas phase CO_2 photoreduction system has increasingly got recognition lately. Although the overall photoactivity (TCEN value) is much lower than the similar dye-sensitized catalyst in liquid phase system, the present TCEN value is relatively high among the gas phase system reported previously as shown in Table S3.[1-6]

Photoelectrochemical properties of ZnPy-TiO_2

To better understand of the charge transfer and electron injection, the photocurrent responses, the time-resolved PL spectra and electrochemical impedance spectra (EIS) spectra are taken out on the pristine TiO_2 and 1.0% ZnPy-TiO_2 films. As shown in Fig. S10a, the photocurrent response of 1.0% ZnPy-TiO_2 is much stronger than the pristine one, which can be ascribed to the fast charge transfer of ZnPy to TiO_2 and the efficient visible light absorption of ZnPy. Moreover, the time-resolved PL spectra also support the charge transfer from ZnPy to TiO_2 Fig. S10b. Under 375 nm laser exciter, ZnPy and TiO_2 are both excited, and the lifetime (τ_n') of ZnPy-TiO_2 is 7.78 ns, much longer than that (1.55 ns) of the pristine one as shown in Table S4. This prolonged lifetime is due to the ZnPy excitation and the consequent charge transfer from ZnPy to TiO_2.[9,10]

Typically, the Nyquist diagrams of the EIS shown in Fig. S11a present two semicircles. The semicircle in high frequency region can be ascribed to the charge transfer resistance (R_1) at the redox electrolyte/Pt counter electrode interfaces; and the semicircle in middle frequency region is related to the resistance (R_2) of the accumulation/transport of the injected electrons within TiO_2 film and the charge transfer across either the TiO_2/redox electrolyte or the FTO/TiO_2 interfaces; R_s (the initial point of Nyquist plot) represents the serial resistance which is determined by the sheet resistance between TiO_2 substrate and the conductive layers of FTO glass.[11-13] The decreased R_2 values when the irradiation is switched on can be related to the photoinduced electrons partly transferred to the surface, which can easily transport to the electrolyte. As can be seen from Table S4, the R_2 value of 1.0% ZnPy-TiO_2 and the pristine TiO_2 films decreases 23.0% and 17.8% when the irradiation is switched on, respectively. It also confirms the more frequent charge transfer from of ZnPy to TiO_2 in the ZnPy-TiO_2 film, and well matched with the above photoactivity and its assumed mechanism. Moreover, the lifetime (τ_n) of photoinduced electrons

can be determined by the position of the low frequency peak (less than 100 Hz) in the Bode plots (Fig. S11b) through the equation that $\tau_n = 1/(2\pi f)$, where f means the frequency of superimposed AC voltage. The lifetimes of both 1.0% ZnPy-TiO_2 and the pristine TiO_2 films can be basically maintained before/after the irradiation switched on. Hence, it can be concluded that the electron reactions of CO_2 photoreduction is on the active sites of TiO_2 surfaces. As a summary, the charge transfer of ZnPy-TiO_2 is that the excited ZnPy molecules inject electrons to TiO_2 and then convert CO_2 over the TiO_2 surfaces.

REFERENCES

1 Z. H. Zhao, J. M. Fan and Z. Z. Wang, *J. Clean. Prod.,* 2007, **15**, 1894.

2 J. Mao, T. Y. Peng, X. H. Zhang, K. Li, L. Q. Ye and L. Zan, *Catal. Sci. Technol.*, 2013, **3**, 1253.

3 J. Mao, T. Y. Peng, X. H. Zhang, K. Li and L. Zan, *Catal. Commun.,* 2012, **28**, 38.

4 H. Zhou, P. Li, J. J. Guo, R. Y. Yan, T. X. Fan, D. Zhang and J. H. Ye, *Nanoscale*, 2015**, 7**, 113.

5 J. G. Yu, J. X. Low, W. Xiao, P. Zhou and M. Jaroniec, *J. Am. Chem. Soc.,* 2014, **136**, 8839.

6 J. Mao, L. Q. Ye, K. Li, X. H. Zhang, J. Y. Liu, T. Y. Peng and L. Zan, *Appl.Catal. B-Environ.,* 2014, **114**, 855.

7 J. Mao, K. Li and T. Y. Peng, *Catal. Sci. Technol.*, 2013, **3**, 2481.

8 E. V. Kondratenko, G. Mul, J. Baltrusaitis, G. O. Larrazabal and J. Perez-Ramirez, *Energy Environ. Sci.,* 2013, **6**, 3112.

9 X. H. Zhang, L. J. Yu, R. J. Li, T. Y. Peng and X. G. Li, *Catal. Sci. Technol.*, 2014, **4,** 3251.

10 X. H. Zhang, L. J. Yu, C. S. Zhuang, T. Y. Peng, R. J. Li and X. G. Li, *RSC Adv.,* 2013, **3**, 14363.

11 J. L. Xu, K. Li, W. Y. Shi, R. J. Li and T. Y. Peng, *J. Power Sources*, 2014, **260**, 233.

12 L. J. Yu, W. Y. Shi, L. Lin, Y. Y. Guo, R. J. Li and T. Y. Peng, *Dyes Pigments*, 2015**, 114**, 231.

13 L. J. Yu, W. Y. Shi, L. Lin, Y. W. Liu, R. J. Li, T. Y. Peng and X. G. Li, *Dalton T.,* 2014, **43**, 8421.